Neurotoxicology 75 (2019) 148–157

Contents lists available at ScienceDirect

Neurotoxicology

journal homepage: www.elsevier.com/locate/neuro

Full Length Article

Huntington's disease associated resistance to Mn neurotoxicity is neurodevelopmental stage and neuronal lineage dependent

Piyush Joshi[a,b], Caroline Bodnya[a], Ilyana Ilieva[b], M. Diana Neely[b], Michael Aschner[c], Aaron B. Bowman[a,b,d,*]

[a] Vanderbilt Brain Institute and Dept. Biochemistry, Vanderbilt University, United States
[b] Depts. of Pediatrics and Neurology Vanderbilt University Medical Center, United States
[c] Depts. of Molecular Pharmacology, Albert Einstein College of Medicine, United States
[d] School of Health Sciences, Purdue University, United States

ARTICLE INFO

Keywords:
Manganese (Mn)
Human induced pluripotent stem cells (hiPSCs)
Cytotoxicity
Neural lineages
Neurodevelopment
Huntington's disease

ABSTRACT

Manganese (Mn) is essential for neuronal health but neurotoxic in excess. Mn levels vary across brain regions and neurodevelopment. While Mn requirements during infanthood and childhood are significantly higher than in adulthood, the relative vulnerability to excess extracellular Mn across human neuronal developmental time and between distinct neural lineages is unknown. Neurological disease is associated with changes in brain Mn homeostasis and pathology associated with Mn neurotoxicity is not uniform across brain regions. For example, mutations associated with Huntington's disease (HD) decrease Mn bioavailability and increase resistance to Mn cytotoxicity in human and mouse striatal neuronal progenitors. Here, we sought to compare the differences in Mn cytotoxicity between control and HD human-induced pluripotent stem cells (hiPSCs)-derived neuroprogenitor cells (NPCs) and maturing neurons. We hypothesized that there would be differences in Mn sensitivity between lineages and developmental stages. However, we found that the different NPC lineage specific media substantially influenced Mn cytotoxicity in the hiPSC derived human NPCs and did so consistently even in a non-human cell line. This limited the ability to determine which human neuronal sub-types were more sensitive to Mn. Nonetheless, we compared within neuronal subtypes and developmental stage the sensitivity to Mn cytotoxicity between control and HD patient derived neuronal lineages. Consistent with studies in other striatal model systems the HD genotype was associated with resistance to Mn cytotoxicity in human striatal NPCs. In addition, we report an HD genotype-dependent resistance to Mn cytotoxicity in cortical NPCs and hiPSCs. Unexpectedly, the HD genotype conferred increased sensitivity to Mn in early post-mitotic midbrain neurons but had no effect on Mn sensitivity in midbrain NPCs or post-mitotic cortical neurons. Overall, our data suggest that sensitivity to Mn cytotoxicity is influenced by HD genotype in a human neuronal lineage type and stage of development dependent manner.

1. Introduction

Manganese (Mn) is a necessary trace element critical for human health and plays a role in many cellular processes. It is a co-factor for enzymes involved in neurotransmitter synthesis and neuronal and glial metabolism (Butterworth, 1986; Erikson and Aschner, 2003). Mn levels in brain tissue are estimated to average 1–2 μg/g dry weight and vary across brain regions (Bowman et al., 2011) with the highest levels of Mn measured in the globus pallidus (2.0 ± 1.2 μg/g) and putamen (Mn, 2.5 ± 0.8 μg/g) (Krebs et al., 2014; Ramos et al., 2014). Excessive exposure to Mn due to occupational activities such as mining and welding can lead to Mn accumulation in basal ganglia dopamine rich regions (Prohaska, 1987). Abnormally high levels of Mn can also lead to a condition known as manganism which is an extra-pyramidal neurological disease and presents symptoms similar to Parkinson's disease (PD) (i.e., cognitive, motor, and emotional deficits) (Aschner et al., 2007; Pharmacol, 1837). The extra pyramidal effects of Mn are believed to be mediated by neurotoxicity in the globus pallidus and basal ganglia structures (Guilarte, 2010; Benedetto et al., 2009).

Levels of Mn across brain regions and neurodevelopmental stage are diverse and it is unclear whether sensitivity of different neuronal subtypes to Mn may be correlated with regional Mn concentrations (Coetzee et al., 2016; Erikson et al., 2002). Indeed, it is the overlap between Mn levels in different brain regions under basal or elevated

* Corresponding author at: School of Health Sciences, 550 Stadium Mall Drive, HAMP 1173A, West Lafayette, IN 47907-2051, United States.
E-mail address: Bowma117@Purdue.Edu (A.B. Bowman).

https://doi.org/10.1016/j.neuro.2019.09.007
Received 5 March 2019; Received in revised form 6 August 2019; Accepted 9 September 2019
Available online 20 September 2019
0161-813X/

exposure conditions and sensitivity of the neurons within those brain regions that presumably contribute to Mn neuropathobiology. There is substantial evidence that both insufficient or excessively high levels of Mn might be harmful to health (O'Neal and Zheng, 2015; Shan et al., 2016; Pfalzer and Bowman, 2017). Mn plays an essential role in neurodevelopment. While some studies show that elevated Mn levels in children leads to behavioral disinhibition, olfactory and motor function, as well as hyperactivity (Ericson et al., 2007; Lucchini et al., 2012), other reports found no correlation between Mn concentrations and brain development (Ode et al., 2015). These inconsistent reports suggest that there are potential differences in Mn cytotoxicity across developmental time and lineage in the brain. Exposure to Mn in prenatal and postnatal periods has been shown to accumulate in striatum and hippocampus (Dorman et al., 2000; Fechter, 1999). Mn neurotoxicity is mediated by altered neurotransmission, neuronal apoptosis, excitotoxicity, and oxidative stress (Coetzee et al., 2016; Fechter, 1999). Many regions and cell types of the brain have been implicated as targets for Mn toxicity including the striatal, cortical and dopamine neurons in both human and animal models (Eriksson et al., 1992; Normandin and Hazell, 2002; Guilarte et al., 2006).

Mn requirements during infanthood and childhood are significantly higher than in adults (Trumbo et al., 2001). Paradoxically, however, elevated levels of Mn have been observed in the aging brain (Ramos et al., 2014). The relationship between brain Mn and Mn-dependent pathways is complicated with evidence of increased activity of Mn-dependent enzymes (e.g. arginase 2), but decreased expression of Mn-dependent enzymes after chronic elevated Mn levels (Bichell et al., 2017). Indeed, the complexities and homeostatic relationship to development and aging of ensuing Mn-requirements are met while avoiding Mn toxicity are not well defined as recently reviewed by us (Pfalzer and Bowman, 2017). Interestingly, studies in rodent models have shown that at young ages Mn toxicity does not lead to cognitive impairment; however, adult ages show a decline in cognitive and behavioral outcomes (Cordova et al., 2013; Fu et al., 2016; Su et al., 2016). Thus, Mn homeostasis is important for brain development and deficient regulation of Mn homeostasis may impair neurodevelopment or lead to neuronal pathophysiology and disease.

HD is an autosomal dominant neurodegenerative disease in which patients exhibit cognitive, behavioral, psychological, and movement dysfunction. It is caused by expansion of the CAG repeat in the huntingtin (Htt) protein, and age of onset is inversely correlated with the number of repeats (Wexler, 2004). There is compelling evidence that environmental factors/modifiers play a role in determining age of onset, one such environmental factors may be Mn (Correia et al., 2015; Friedman et al., 2005). Previous studies in several different HD models have shown decreased cellular Mn-uptake supporting the hypothesis that HD is associated with neuronal cell type specific deficit in Mn bioavailability (Bichell et al., 2017; Horning et al., 2015). Mn has been shown to play a role in cell signaling pathways such as ATM-p53, pathways that are altered in experimental models of HD (Tidball et al., 2015).

Here, we present the first study assessing Mn cytotoxicity in different human neuronal lineages and different neuro-developmental stages of control and HD patient hiPSC-derived striatal, cortical and developing mesencephalic dopaminergic neurons. Cellular mechanisms of Mn neurotoxicology are not fully understood and the dose response relationships of Mn toxicity are elusive. Over the course of this study, we discovered that there is a strong effect of media-type on Mn toxicity, such that an accurate comparison of Mn cytotoxicity between developing human neuronal lineages cannot be done using the lineage specific medias that are optimal for human neuronal differentiation protocols. Thus, we tested instead whether the HD genotype affects Mn-induced cytotoxicity between cortical, striatal, and midbrain neural lineages across developmental stages comparing control and HD patient derived cells.

2. Materials and methods

2.1. hiPSCs Cell Culture

hiPSCs lines derived from five healthy control subjects (CA30, CC3, CD2, CD12, CE6, CX3) and four HD patients (HD58-3, HD70-2, HD70-11, HD180-6) were used, which included both males and females and have been described and validated in detail elsewhere (Tidball et al., 2016). hiPSCs were maintained in mTeSR1 medium (StemCell Technologies, Vancouver, BC) on Matrigel (BD Biosciences, San Jose, CA) coated six-well plates. hiPSCs were dissociated by incubating for 10 min in Accutase (Innovative Cell Technologies, San Diego, CA), then centrifugated and resuspended in mTeSR1 with 10 μM ROCK inhibitor Y-27632 (Tocris) and replated at 100,000 cells/ml. Neural differentiation was started after the hiPSCs cultures reached 100% confluency. All Mn exposures for hiPSCs were conducted after they reached 90–100% confluency.

2.2. Cortical neural differentiation

Cortical neural induction was performed following the dual SMAD protocol published by Chambers et al., except that LDN193189 (Stemgent Cat. N. 04-0074) at 0.4 μM was used instead of noggin. SB431542 (10 mM) was purchased from (Stemgent Cat. N.04-0010) (Chambers et al., 2009; Neely et al., 2012; Di Pardo et al., 2017) (Fig. 1B). Neuralization medium consists of 410 ml Knockout DMEM/F12 (Invitrogen #12660), 75 ml Knockout Serum (Invitrogen # 10828), 5 ml μl β-mercaptoethanol (Sigma # M3148) and N2 medium which consists of 500 ml DMEM/F12 (Invitrogen #10565-018, + glutamax), 0.775 g D-Glucose, and 5 ml N2 supplement (Thermo Fisher Scientific#17502048). After 10 days of neural induction, neural differentiation was initiated as reported by Shi et al (Shi et al., 2012). Briefly, cells were switched to media composed of 50% N2 CTX medium and 50% B27 Neurobasal medium. N2 CTX medium: 500 ml DMEM/F12 + glutamax (Invitrogen #10565-018, + glutamax), 5 ml N2 supplement (Invitrogen #17502-048), 5 ml non-essential amino acids (100x stock, Invitrogen # M7145), 10 ml Pen/Strep (100 x stock; Mediatech # 30-002-Cl), 3.5 μl β-mercaptoethanol (Sigma # M3148). B27 Neurobasal medium: 500 ml Neurobasal medium (Life Technologies #21103-049), 10 ml B27 supplement (Life Technologies #17504044), 5 ml Glutamax (Life Technologies #10565042). The media for day 11 cortical exposures consists of 25% neuralization media and 75% N2 media with SB431542 (10 mM) and LDN193189 (0.4 μM) (Fig. 1B). Additional details and validation of this differentiation method have been previously reported (Neely et al., 2012; Di Pardo et al., 2017; Brown et al., 2016).

2.3. Striatal neural differentiation

Striatal differentiation (Fig. 1C) was conducted for 11 days via the same dual SMAD neural induction protocol using LDN (4 μM) (Stemgent Cat. N. 04-0074) and SB431542 (10 μM) (Stemgent Cat. N.04-0010), but, in addition purmorphamine (0.65 μM) (Stemgent, Cambridge, MA) (Tidball et al., 2015; Bryan et al., 2017) was added to pattern striatal NPCs. The media for day 11 striatal exposures consists 100% N2 media purmorphamine (0.65 μM) (Fig. 1C). Additional details and validation of this differentiation method have been previously reported.

2.4. Midbrain neural differentiation

Midbrain dopamine (DA) differentiation was performed as described (Kriks et al., 2011) except that LDN was used at 0.4 μM (Stemgent Cat. N. 04-0074) (Neely et al., 2017; Kumar et al., 2014). All NPCs were replated at 300,000 cells/ml on day 8 and early neurons were replated at 500,000 cells/ml on day 22 for all relevant exposures.

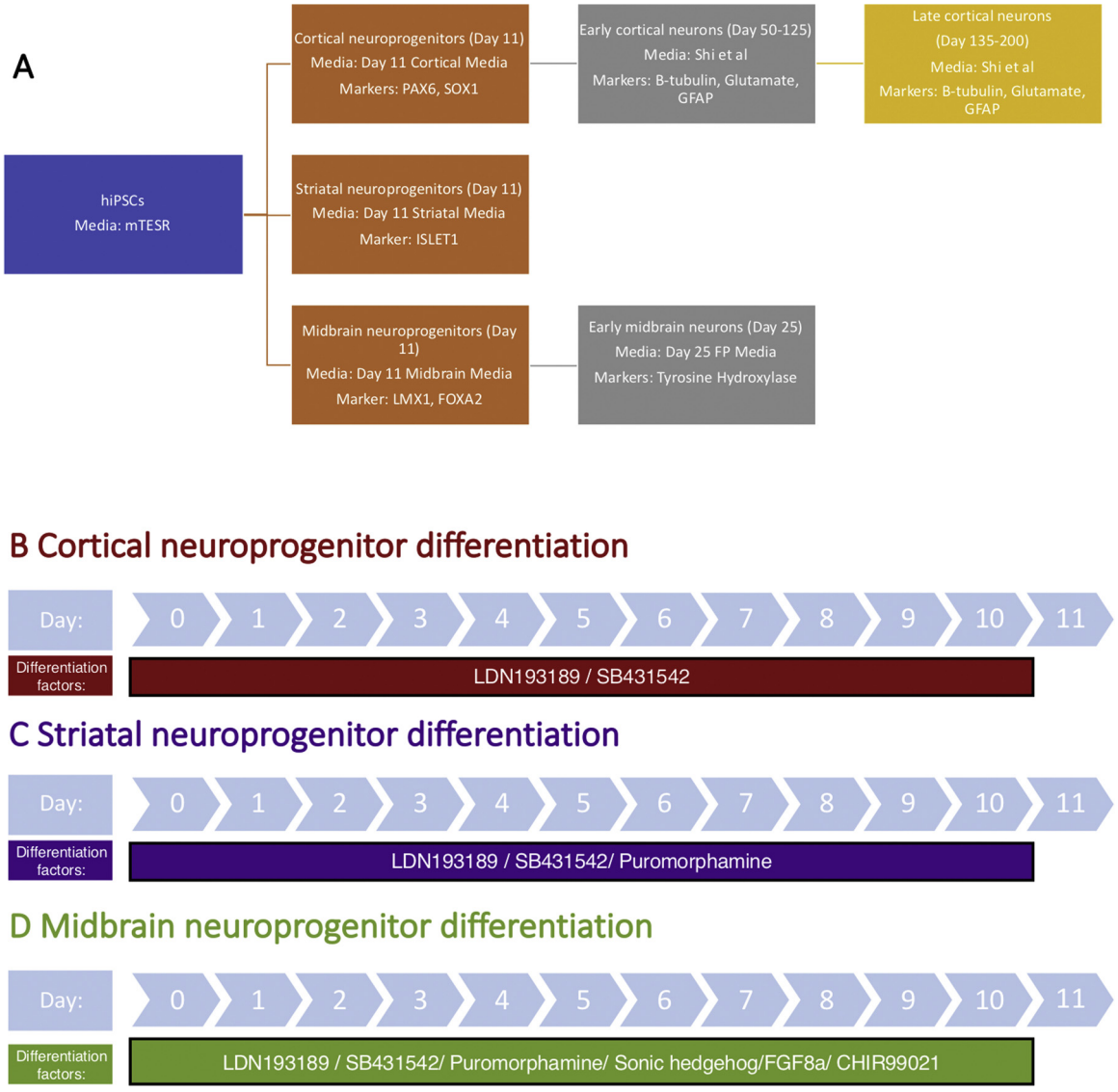

Fig. 1. Summary data of Mn cytotoxicity in human neuronal lineages. (A) Differentiation of hiPSCs to NPCs and neurons. (B–D) Protocol summaries for differentiating three different neuroprogenitor lineages.

The media for day 11 midbrain exposures consists of 25% neuralization media and 75% N2 media with CHIR99021 (3 mM) and LDN193189 (0.4 μM) (Fig. 1D). The media for day 25 early midbrain neurons consists of 100% neurobasal media + glutamax with these compounds: BDNF (20 ng/ml), GDNF (20 ng/ml), TGFb3 (1 ng/ml), dcAMP (0.5 u M), DAPT (10μM), and ascorbic acid (200μM). Additional details and validation of this differentiation method have been previously reported (Neely et al., 2017).

2.5. Validation of lineage differentiation

Supplemental Fig. 1 shows an example confirmation of expression of lineage specific markers at Day 11 for cortical, striatal, and midbrain NPCs. All cells to be analyzed were plated into 96 well plates (Greiner Bio-One, Monroe, North Carolina, μclear) and immunofluorescence was performed. Cells were fixed in 4% paraformaldehyde (PFA) in PBS solution for 20 min at room temperature, the cells were permeabilized with 0.2% Triton X-100 for 20 min, and incubated in PBS containing 5% donkey serum (Jackson ImmunoResearch, West Grove, Pennsylvania) and 0.05% Triton-X (Sigma) overnight at 4 °C. The following day, primary antibodies (Pax6, Sox1, LMX1a, FOXA2, and ISLET1 (Tidball et al., 2015; Neely et al., 2017)) were added and incubated overnight at 4 °C. Secondary antibodies were added the next day and plates were imaged using a Zeiss ObserverZ1 microscope and AxioVs40 software (version 4.7.2).

2.6. Mouse striatal cell model system

Immortalized, wild-type STHdh[Q7/Q7] (abbreviated to STHdh) murine striatal cell lines from Coriell Cell Repository (Cambden, NJ) were cultured in Dulbecco's Modified Eagle Medium (D6546, Sigma-Aldrich, St. Louis MO). DMEN was supplemented with 10% Fetal Bovine Serum (FBS) (Atlanta Biologicals, Flowery Branch, GA), 2 mM GlutaMAX (Life Technologies, Carlsbad, CA), Penicillin-Streptomycin, 0.5 mg/ml G418 Sulfate (Life Technologies, Carlsbad, CA), MEM non-essential amino acids solution (Life Technologies, Carlsbad, CA), and 14 mM HEPES (Life Technologies, Carlsbad, CA). The STHdh cells were incubated in 33°and 5% CO2 and passaged by utilizing 0.05% Trypsin-EDTA solution (Life Technologies, Carlsbad, CA). The STHdh cells were plated at 80,000 cells/ml (Williams et al., 2010a, b) and were cultured on Matrigel to mimic the plate conditions of the neural lineages. Twenty-four hours after replating, cells were exposed to different human neuronal differentiation media types to test for media-dependent effects on Mn cytotoxicity.

2.7. Mn exposures

hiPSCs were replated at 100,000 cells/ml 3 days before start of 24 -h Mn exposure. All lineages of day 11 NPCs were replated on day 8 at 300,000 cells/ml and cortical neurons that had undergone neuronal differentiation were replated at different stages of differentiation at 500,000 cells/ml. Mesencephalic dopaminergic neurons were replated on day 22 at 500,000 cells/ml as described. All cells were plated into Matrigel coated 96 well plates and exposed to Mn in the lineage and developmental-stage specific medium. ROCK inhibitor was removed 24 h prior to all Mn exposures in all human derived cell types and all cells were exposed for 24 h in Mn. For the STHdh cells, they were plated at 80,000 cells/ml on Matrigel and exposed 24 h later with Mn in the different human neuronal differentiation media.

2.8. Quantification of net cellular Mn accumulation

Quantification of intracellular Mn levels was preformed using the validated Cellular Fura-2 Mn Extraction Assay (CFMEA) exactly as described (Kwakye et al., 2011a, b).

2.9. Cell viability assay

After the 24 -h exposure to Mn exposure, 20 µl of Cell Titer Blue reagent from Cell Titer Blue assay (Promega, G8081) was added to each well of 96 well plate. Cell lysis buffer (10% Triton in PBS) was added to some wells to provide background fluorescence for zero percent viability. In this assay, live cells reduce resazurin to resorufin, whose fluorescence correlates with the number of viable cells. The fluorescence was measured using excitation of 570 nm and emission of 600 nm by using a Beckman coulter DTX 880 multimode plate reader (Beckman Coulter, Brea, California). The sample size (n) refers to the number of independent differentiations of subject lines within each group (i.e. HD or control), with the number of independent hiPSC lines (see above for the list of lines within each group) that contribute to this total sample size for each experimental group stated in the figure legend. Multiple reads at different time points after addition of the cell titer blue reagent were conducted for each cell type and every experiment to optimize this assay for duration to avoid saturation of signal and ensure comparable cell titer blue signal strength across cell types and media types (Supplementary Table 1). We sought to achieve a background subtract signal strength for the vehicle control samples of each experiment between 18000–60000 fluorescent units depending on cell type. More information about the assay can be found here, as previously described (Joshi et al., 2018).

2.10. Strategy for determining concentration response curves

To accurately determine Mn cytotoxicity in hiPSCs and derived lineages, full concentration curves to Mn were conducted (Supplemental table 2), limited to 8 different concentrations to allow for 3–4 technical replicates in our plating design. The majority of concentrations of Mn selected were aimed at clustering close to LC50 values to enable accurate calculations across lineages. Though we also sought to ensure at least one low concentration with minimal cytotoxicity (> 85% survival) and one high concentration with maximal cytotoxicity (< 15% survival). When necessary to allow for a sufficient range of cell toxicity on either side of the experimentally determined LC50, we adjusted the Mn concentrations used in subsequent trials if there was limited range of cell death using the initial exposure concentrations (typically 0–1000 µM, though later tested lineage stages were informed by prior curves as to the optimal starting exposure range). Supplemental table 2 provides all survival data by experiments across all concentration response curves. This experimental design was established to ensure optimal ability to calculate an LC50 value across all experiments. However, to ensure a consistent comparison across all response curve experiments, a 500 u M Mn exposure was used across all lineages.

2.11. Statistics

Statistical analyses were performed using Prism software version 8.0 (GraphPad, La Jolla, CA) and Excel (Microsoft, Redmond, WA). XY analyses (non-linear regression (curve fit)) test with inhibitor vs. normalized response- variable slope was conducted. This model does not assume a standard slope but fits the hill slope from data. Lethal concentration 50 (LC50), R square, and degrees of freedom were calculated for survival of all cell types and 95% confidence intervals were plotted. LC50 is the dose of Mn at which 50% of the cells were killed in a 24 -h exposure. Non-overlapping calculated confidence intervals were used to identify statistically significant differences in control and HD. Pearson correlation analysis was performed using Prism software, with two-tail P values and Pearson r values reported. Two-way ANOVA was performed using Prism software with a repeated measure design by each experimental replicate, Sidak's multiple comparisons tests were used for binary post hoc comparisons.

3. Results

3.1. Neuronal lineages derived from hiPSCs show differences in Mn sensitivity by lineage and developmental stage

Neural lineages derived from control subject and HD patient hiPSCs were exposed to Mn for 24 h in stage-appropriate media (Fig. 1A). Based on established protocols (Tidball et al., 2015; Chambers et al., 2009; Neely et al., 2012; Kriks et al., 2011), we differentiated cells along three different lineages: cortical glutamatergic, striatal GABAergic projection NPCs, and midbrain dopaminergic. Each lineage requires different types of base media, supplements, and differentiation factors during in vitro differentiation into target NPCs or neurons (Fig. 1B-D). We first examined the cytotoxicity in control subject hiPSC-derived NPCs and neurons to Mn exposure in the lineage and stage appropriate media for all three lineages to determine relative sensitivities to Mn cytotoxicity. The incubation times for Cell Titer Blue assay were optimized for different cell types to match for similar range of values (Supplementary Table 1). Control subject hiPSC and hiPSC-derived NPCs plotted showed a difference in relative sensitivity to Mn, with the striatal NPCs showing the greatest sensitivity, while cortical and midbrain NPCs were relatively more resistant to Mn toxicity at a comparable stage of development (Table 1). The early midbrain neurons are the most resistant, with LC50 values almost double that of the early cortical neurons (Table 1). While this may be noteworthy, given the relatively high accumulation of Mn in the midbrain upon in vivo exposures (Pharmacol, 1837; Tidball et al., 2015), subsequent analysis reported here next strongly suggests that the majority of lineage differences are largely due to differences in the lineage-specific media itself rather than cell autonomous differences.

3.2. No difference in the sensitivity of day 11 neuronal lineages when media type is controlled

Differentiation of hiPSCs down distinct neural lineages requires the sequential exposure to specific media-types and supplemented small molecules. Mn exposures were performed in the media appropriate for each lineage/stage of neural development. Thus, we sought to test whether differences in Mn cytotoxicity could also be influenced by the different lineage-specific media as well as differences in the cell autonomous lineage-specific phenotypes. To test this, we differentiated hiPSCs cortical, striatal, and midbrain NPCs to day 11, and exposed each to 200µM Mn in all three lineage-specific media for 24 h side-by-side to control for each differentiation. Two-way repeat measure ANOVA matched by experimental set (n = 4 experimental sets)

Table 1
LC50 concentration (report in μM Mn) and hill slope coefficients after 24 -h Mn exposures. Significant differences between control and HD values are indicated by (*) and bold text for the HD value reported.

	hiPSCs	Day 11 Cortical NPCs	Day 11 Striatal NPCs	Day 11 Midbrain NPCs	Early Midbrain Neurons (Day 25)	Early Cortical Neurons (Day 50-125)	Mature Cortical Neurons (Day 135-200)
LC50-Control	520	1448	559.8	1639	3572	1871	2086
95% confidence interval	"502.1 to 536.9"	"1322 to 1597"	"505.5 to 615.2"	"1463 to 1841"	"2672 to 5683"	"1533 to 2315"	"1629 to 2761"
LC50- HD	**586***	**2657***	**777.6***	1593	**1165***	2445	2498
95% confidence interval	"542.6 to 629.2"	"2249 to 3248"	"707.2 to 855.5"	"1417 to 1803"	"956.5 to 1450"	"1946 to 3151"	"1779 to 3773"
Hill Slope- Control	7.789	1.737	2.329	1.650	0.9989	1.63	3.107
95% confidence interval	"5.559 to 11.23"	"1.512 to 1.996"	"1.86 to 2.961"	"1.376 to 1.979"	"0.7034 to 1.362"	"1.287 to 2.113"	"1.849 to + infinity"
Hill Slope- HD	**2.738***	2.645	2.269	1.482	0.865	1.273	1.304
95% confidence interval	"2.081 to 3.721"	"1.554 to 7.085"	"1.784 to 2.909"	"1.245 to 1.76"	"0.6755 to 1.085"	"0.9922 to 1.628"	"0.8381 to 2.015"

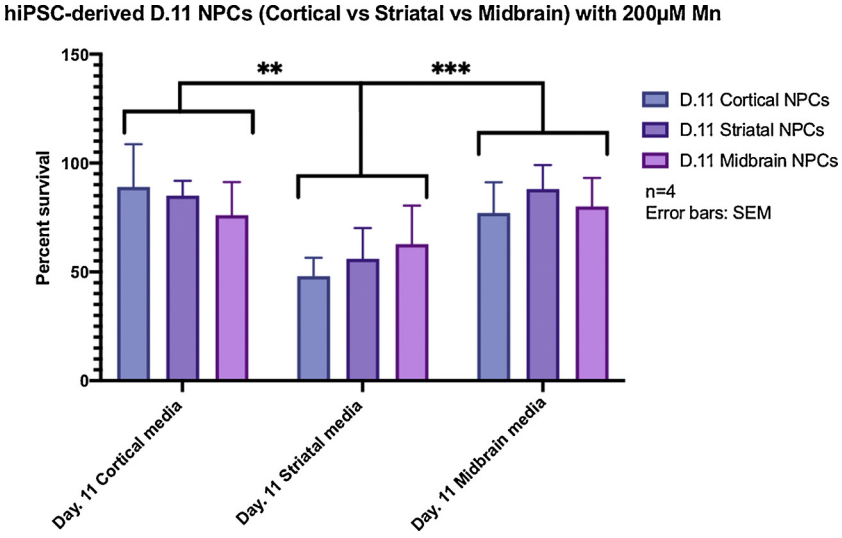

Fig. 2. No difference in the sensitivity of day 11 NPCs when media type is controlled. NPCs were generated from hiPSCs into cortical, striatal, and midbrain day 11 NPCs and exposed to 200 μM Mn for 24 h. Cell titer blue assay was conducted in opposing medias to assess the effect of media on lineage. Two-way repeated measure ANOVA matched by experiment set showed a significant effect of media. Post-hoc Tukey's multiple comparison analysis demonstrated all three NPC lineages were more sensitive in day 11 striatal media. **P value is 0.006 and ***P value is < 0.0001.

demonstrated a significant effect of media type ($F_{(1.256,\ 11.31)} = 17.70$, $P = 0.0009$), but no difference by neuronal lineage, or a lineage by media type interaction effect (Fig. 2). Post-hoc Tukey's multiple comparison analysis revealed that all lineages were more sensitive after 24 -h exposure to 200μM Mn in Day 11 striatal media versus either the Day 11 cortex media or Day 11 midbrain media. Examination of the data show that consistent with the ANOVA result of no significant effect by lineage, there is no substantial difference in cytotoxicity across the three lineages when compared in exposures to a single media type. Thus, for Day 11 lineages, this strongly suggests that our LC50 values showing that the striatal lineage is more sensitive than the cortical or midbrain lineage at Day 11 (Table 1) is driven almost exclusively by the striatal lineage media.

Cytotoxicity and net Mn uptake in STHdh mouse cell line show a strong correlation between lineage/stage specific media type and observed LC50 value of the corresponding hiPSC-derived neural lineage/stage

After observing no difference in lineage sensitivity to Mn if media-type was controlled for, we choose to test media effects in a non-human immortalized mouse striatal cell line. This is the same line in which our lab first observed a Mn uptake phenotype in HD cells. The wild-type mouse striatal cell line, STHdh, is known to have high sensitivity to Mn cytotoxicity with substantial cell death at even 100μM Mn for 24 h in its normal bovine-serum containing DMEM media (Tidball et al., 2015; Williams et al., 2010a). We reasoned that if media-type influenced cytotoxicity significantly then the observed survival after Mn exposure in this non-human striatal cell line across the different media-types may correlate with the observed LC50 in the same media-type observed for the hiPSC-derived neuronal lineages/stages. The STHdh cells were plated and exposed for 24 h to 500μM Mn, a higher dose to account for the supplement rich human medias, in all the different media-types used for each neuronal lineage/stage. We measured cell survival by cell titer blue assay then compared these values to our measured control LC50 values (see Table 1) in the corresponding human neuronal lineage/stage for that media. We also measured total Mn accumulation after the same 24 -h exposures by the CFMEA assay and compared these values to the measured hiPSC neural lineage LC50 values. Cytotoxicity measurements and CFMEA for cellular Mn levels indeed showed that type of media is significantly correlated with LC50 values in the human cell lineages (Fig. 3A-B). To determine if the degree of Mn uptake in the different media types was a strong driver of the observed cytotoxicity, in the STHdh line itself, we measured the correlation between Mn-uptake (CMFEA assay) and cell survival in the STHdh cell line and also observed that ~85% of the variance in cell survival could be explained by the variance in net Mn accumulation (Fig. 3C). These data from a non-human immortalized neuroprogenitor cell line argue that a substantial degree (80–90%) of the observed differences in Mn cytotoxicity between the different human neuronal lineages and developmental stages (Table 1) can be explained by the influence of the specific media-type on Mn transport. Thus, analysis of Mn neurotoxicity across lineages cannot be assessed due to the different media requirements of differentiation.

Further work is needed to determine the media composition responsible for the effects on Mn cytotoxicity. But on possibility is that

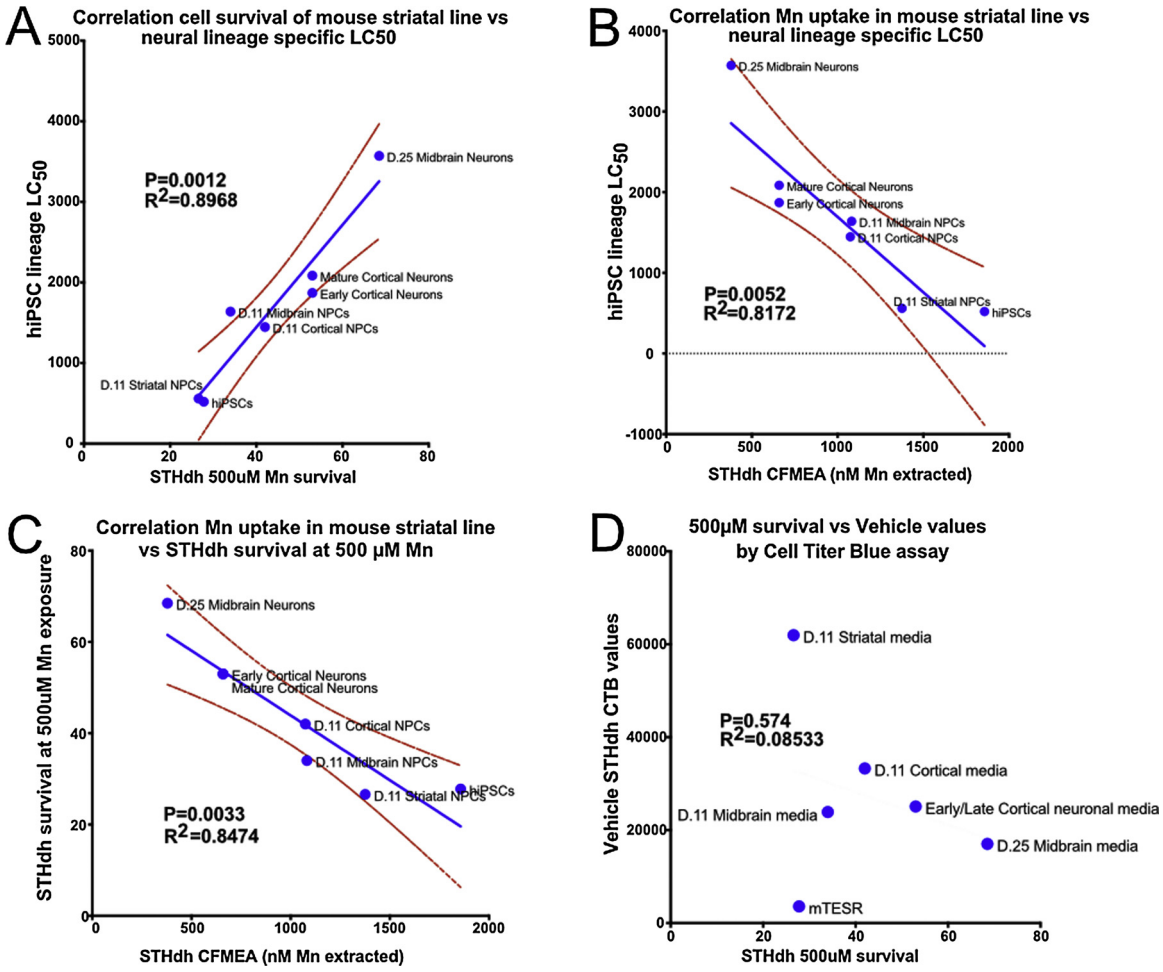

Fig. 3. Cytotoxicity and net Mn uptake in a high sensitivity to Mn cell line STHdh exposure to lineage and stage specific media was significantly correlated with the observed LC50 values in the human neuronal lineages. The immortalized mouse striatal cell line STHdh was incubated with the same human neural differentiation lineage specific media with and without 500µM Mn. Cell death was quantified by cell titer blue (CTB) and net Mn uptake was quantified by CFMEA. The measured LC50 associate with the human developmental stage for that media significantly correlated with the percent cell survival of the striatal cell line in the same media (A), and inversely correlated with the total intracellular Mn extracted from the striatal cell line (B). (C) Further the degree of cell death in the mouse striatal cell line in the corresponding human neuronal lineage media inversely correlated with the total intracellular Mn extracted from the striatal cell line in the same media. (D) Absolute cell titer blue signal for the vehicle exposed cell cultures were plotted against the survival rate of the 500µM Mn treated cultures in the same media, no significant correlation was observed. (A–D) Pearson correlations were calculate for each comparison, the computed linear relationship is indicated with a blue line with its 95% confidence interval boundaries marked with red dashed lines; the R^2 and associate p-value are report for each panel.

media type could influence cell density and growth measurements, as different media-type may affect the cell's ability to reduce resazurin to resorufin, the key reaction in the Cell Titer Blue assay, we examined the correlation between the observed cytotoxicity at 500µM Mn and the background-subtracted raw cell titer blue assay values for the vehicle-only media exposure between media-types (Fig. 3D). Pearson correlation analysis failed to detect a significant relationship. Thus, the observed LC50 values of different neuronal lineages/stages was significantly correlated with Mn-cytotoxicity and net Mn accumulation in the STHdh mouse striatal neuroprogenitor cell line using only the associate cell culture media of that lineage/stage. However, this effect does not appear to be due to changes in the observed cell growth and cell density as measured by the cell titer blue viability assay. Therefore, it remains unknown whether Mn sensitivity is altered across these neuronal lineages and/or developmental stages.

3.3. HD genotype has differential influence on Mn cytotoxicity dependent on neural lineage

While the above findings suggested comparison across lineage type is not possible. Comparison of different genotypes within a specific lineage and stage where the media type is identical is valid. We have previously reported that the HD genotype confers resistance to Mn cytotoxicity in striatal NPC (Tidball et al., 2015). Thus, we compared Mn cytotoxicity in control and HD day 11 cortical, midbrain and striatal NPCs performing a full concentration response curve under a 24 -h Mn exposure paradigm. While the HD genotype was associated with resistance to Mn cytotoxicity in cortical and striatal NPCs, this genotype-dependent difference was not observed for the midbrain NPCs (Table 1 and Fig. 4A-C). Thus, consistent with our previous reports, we observed that the HD genotype confers resistance to Mn in striatal NPCs (control LC50 = 559.8 µM vs HD LC50 = 777.6 µM; Table 1 and Fig. 4B) and interestingly this HD genotype-associated resistance showed an even greater magnitude in the cortical NPC lineage (control LC50 = 1448 µM vs HD LC50 = 2657 µM; Table 1 and Fig. 4A). Thus, the HD genotype is associated with protection against Mn cytotoxicity in a neural lineage-dependent manner across NPCs of similar developmental stage.

3.4. Maturation of the cortical lineage eliminates the influence of HD genotype on Mn cytotoxicity

After studying the effects of Mn on the viability of NPCs, we

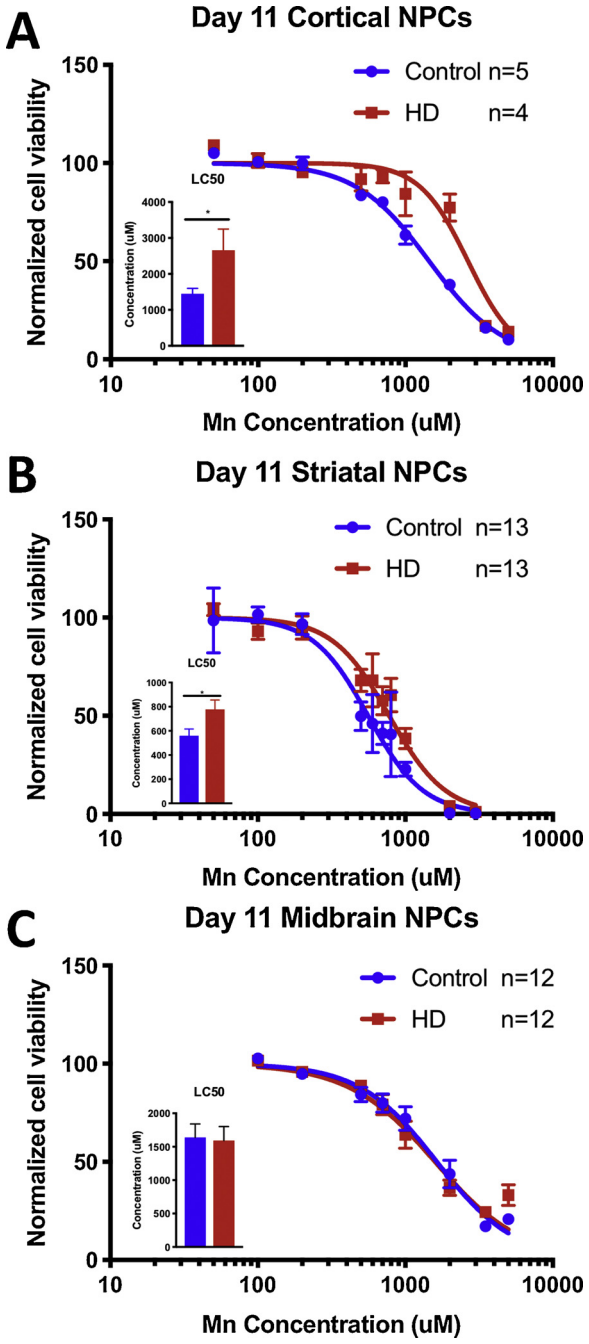

Fig. 4. Assessing sensitivity of Mn in three different NPC lineages. The Cell Titer Blue assay was used to determine cell viability. Error bars represent the 95% confidence interval for LC50 values and hill slopes. (A) Control n = 5 biological replicates (CC3 = 3, CX3 = 2) across 3 experimental sets with R^2 = 0.9588 and degrees of freedom (Df) = 32. HD n = 4 biological replicates (HD58-3 = 1, HD70-2 = 3) across 3 experimental sets with R^2 = 0.7989 and Df = 26. (B) Control n = 13 biological replicates (CC3 = 5, CD2 = 1, CD12 = 3, CE6 = 4) across 7 experimental sets with R^2 = 0.8431 and Df = 92. HD n = 13 biological replicates (HD58-3 = 6, HD70-2 = 7) across 7 experimental sets with R^2 = 0.8137 and 92 Df. (C) Control n = 12 biological replicates (CC3 = 6, CD12 = 4, CE6 = 2) across 3 experimental sets with R^2 = 0.8198 and Df = 94. HD n = 12 biological replicates (HD58-3 = 6, HD70-2 = 6) across 3 experimental sets with R^2 = 0.8186 and Df = 94.

assessed whether more mature hiPSC-derived cortical (glutamatergic) neurons display a similar HD-genotype-dependent effect on Mn sensitivity. Interestingly in the day 50–125 and day 135–225 of differentiated cortical neurons we observed no significant difference in the LC50 for Mn between control and HD genotype (control LC50 = 1871 μM vs HD LC50 = 2445 μM; Table 1 and Fig. 5A and control neurons LC50 = 2086 μM vs HD LC50 = 2498 μM; Table 1 and Fig. 5B). Additionally, the 95% confidence interval of the hill slope coefficients of the concentration response curve were overlapping (Table 1). Thus, for the cortical lineage the HD genotype associated resistance to Mn cytotoxicity is confined to the NPC stage and is lost as they develop (Fig. 4A versus Fig. 5).

3.5. Maturation of the midbrain lineage is associated with inverse response of HD genotype to Mn cytotoxicity

Interestingly, we did not observe an HD genotype-associated difference in Mn-sensitivity in NPCs of the midbrain (dopaminergic) lineage (Fig. 4C). Here we assessed the Mn-sensitivity of more mature control and HD midbrain (dopaminergic) neurons. Day 22 (early) midbrain neurons were replated, exposed for 24 h to Mn starting on day 24 and cell viability quantified on day 25. Early midbrain control neurons were significantly more resistant to Mn cytotoxicity (LC50 = 3572 μM) than early HD midbrain neurons (LC50 = 1165 μM); thus, opposite to the cortical and striatal HD NPCs which were more resistant to Mn than their control counterparts early HD midbrain neurons show greater Mn sensitivity than the control neurons (Table 1 and Fig. 6). The early midbrain lineage is the only one in which we observed higher Mn-sensitivity in the HD genotype.

3.6. HD genotype influences the shape of the Mn cytotoxicity concentration response curve in hiPSCs

To better understand the developmental timing of the HD genotype effects on Mn cytotoxicity we evaluated the genotype-dependent Mn sensitivity of the hiPSCs from which all the neurons used in this study were differentiated. hiPSCs from control subjects and HD patients were exposed to a Mn concentration response curve for 24 h in stem cell media (mTeSR). During the 24 -h exposure, cell titer blue reagent was added to each well and incubated at 37 °C for the last 2 h. HD hiPSCs lines were less Mn-sensitive than the hiPSC from control subjects (Table 1 and Fig. 7), LC50 values for controls are 525 μM Mn whereas LC50 for HD patient lines is 580 u M Mn and Hill slope coefficients were non-overlapping. The significant difference in Hill slope due to the HD genotype is observed as a flattening of the curve at higher Mn exposures which suggests that the conferral of resistance to Mn cytotoxicity by the HD genotype is more effective at higher concentrations, e.g. above 500 μM Mn in the hiPSC lines. Although the HD resistance phenotype is observed in hiPSCs, the differences between HD and control Mn sensitivities is larger in day 11 cortical and striatal NPCs than the hiPSCs, while it appears to get lost during the neural induction to the midbrain NPCs.

4. Discussion

We report here the observation that Mn cytotoxicity sensitivity of hiPSC-derived NPCs and neurons is different depending on the neuronal lineage as well as developmental stage. Our results demonstrate that degree of Mn-induced cytotoxicity in hiPSC-derived NPCs and neurons is determined not only by cell autonomous traits, specifically genotype, but is also strongly dependent on the extrinsic environmental factors (i.e. the culture media). To test this, hiPSCs were differentiated into cortical, striatal, and midbrain NPCs to day 11, and exposed to 200μM Mn in all three lineage-specific media for 24 h side-by-side to control for each differentiation. Our results showed that the increased sensitivity of the striatal lineage seen in the concentration response curves is driven by the striatal lineage media itself (Fig. 2, Table 1). Furthermore, we demonstrate here that the Mn-sensitivity of the STHdh cell line varied significantly with the type of medium the cells were exposed in and that the culture media dependent cytotoxicity of STHdh cells strongly

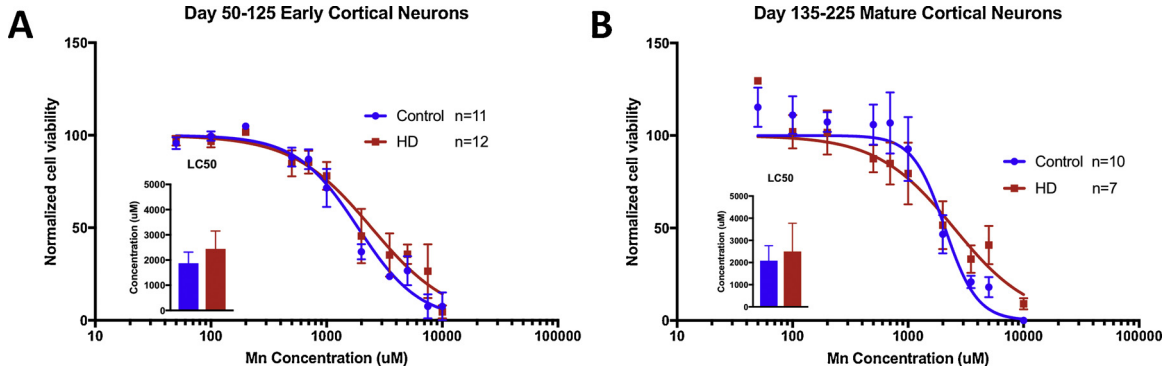

Fig. 5. Mn sensitivities in early and mature control and HD cortical neurons are not different. The Cell Titer Blue assay was sued to quantify cell viability. Error bars represent the 95% confidence interval for LC50 values and hill slopes. (A) Control n = 11 biological replicates (CC3 = 6, CD2 = 3, CE6 = 2) across 6 experimental sets with R^2 = 0.7839 and Df = 76. HD n = 12 biological replicates (HD58-3 = 5, HD70-2 = 6, HD180-6 = 1) across 6 experimental sets with R^2 = 0.6829 and Df = 84. (B) Control n = 10 biological replicates (CC3 = 4, CD2 = 2, CD12 = 1, CE6 = 2, CX3 = 1) across 6 experimental sets with R^2 = 0.549 and Df = 76. HD n = 7 biological replicates (HD58-3 = 2, HD70-2 = 2, HD70-11 = 1, HD180-6 = 1) across 6 experimental sets with R^2 = 0.5457 and Df = 53.

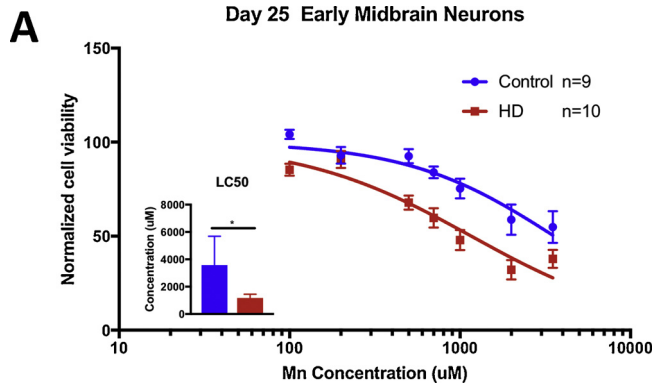

Fig. 6. Mn sensitivity is significantly higher in HD early midbrain neurons than their control counterparts. Error bars represent the 95% confidence interval for LC50 values and hill slopes. Control n = 9 biological replicates (CC3 = 5, CD12 = 1 CE6 = 3) across 3 experimental sets with R^2 = 0.54 and Df = 67. HD n = 10 biological replicates (HD58-3 = 5, HD70-2 = 5) across 3 experimental sets with R^2 = 0.7217 and Df = 74.

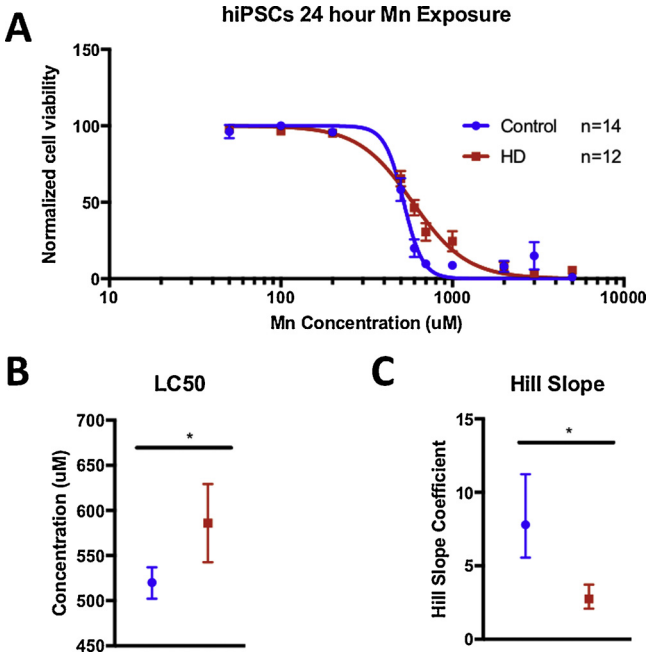

Fig. 7. Mn sensitivity in human induced pluripotent stem cells. (A–B) There was a statistically significant difference between controls and HD patient lines calculated LC50 values. (A) Concentration response curves are shown for Mn exposure versus normalized viability, error bars = SEM. (B) LC50 concentration values are reported for both controls and HD lines. Error bars represent the 95% confidence interval for LC50 values. (C) Hill slopes for all hiPSCs were non-overlapping. Error bars represent the 95% confidence interval for hill slopes. Control n = 14 biological replicates (CC3 = 7, CX3 = 5, CD2 = 1, CE6 = 1) across 7 experimental sets with R^2 = 0.9082 and Df = 96. HD n = 12 biological replicates (HD58-3 = 5, HD70-2 = 7) across 7 experimental sets with R^2 = 0.8724 and Df = 84.

correlated with experimentally determined LC50 of the hiPSC-derived neuronal lineages exposed to Mn in these same media types. In addition, we also observed a media-dependent Mn-uptake difference in STHdh cells which correlated with the LC50 observed for the hiPSC-derived neuronal lineages in the same media, suggesting that intracellular Mn levels are the predominant determinant of Mn cytotoxicity. This effect of the media on Mn-induced cytotoxicity and cellular Mn levels was unexpectedly strong and responsible for about 80% of the variance.

Based on our previous observations that the HD-genotype confers resistance to Mn cytotoxicity in several different HD models (Bichell et al., 2017; Tidball et al., 2015; Williams et al., 2010b), we assessed the relative Mn sensitivity of HD hiPSC-derived neuronal lineages and observed that HD cortical and striatal but not midbrain NPCS were relatively less sensitive to Mn than their control counterparts (Fig. 4); interestingly this HD-phenotype was not observed in developmentally more mature (> day 25) hiPSC-derived neurons. Thus, the HD-genotype-conferred Mn-resistance is neuronal-lineage and developmental stage dependent.

We report here the discovery that the post-mitotic midbrain dopaminergic lineage shows the opposite effect of the HD genotype, being associated with increased sensitivity to Mn cytotoxicity. This HD Mn sensitivity phenotype was not present in midbrain day 11 NPCs, but just after another 14 days of differentiation there is a clear difference between control and HD Mn sensitivity. These were the only cells we tested in which the controls were more resistant to Mn than their HD counterparts, and future studies into these lineage-specific effects may lead to insight into the role of changes in Mn biology to the selective neuropathology in HD. The transition between these stages is striking since these cells are so closely related and with such a high magnitude difference in their apparent phenotype. Our data suggest that midbrain NPCs actually gain sensitivity to Mn cytotoxicity in HD cells as they mature for day 11 midbrain NPCs to day 25 early post-mitotic dopaminergic neurons, while control cells become more resistant. This result has implications for parkinsonian-like toxicity induced by Mn, manganism. Despite the similarities of the motor phenotype between PD

and manganism, the later presents with insensitivity to levodopa (L-DOPA) and differences in disease progression, which may potentially be explained by selective sensitivity to Mn in neuronal lineages and/or developmental stages (Guilarte and Gonzales, 2015; Kwakye et al., 2015). Specifically, it suggests a developmental specific effect of Mn sensitivity in this lineage, that is altered by the HD genotype. If the developing dopaminergic neuronal lineage becomes more resistant to Mn with maturation (as implied by our observation) then this may partially explain the insensitivity of manganism to L-DOPA treatment. However, as the two media types themselves lead to similar differences in Mn cytotoxicity between D11 and D25 midbrain lineage neurons, thus this requires future investigation.

The novelty of this study lies in our observation that human neuronal cells derived from HD -patient hiPSCs and the hiPSC cells themselves show HD genotype effects on Mn toxicity dependent on neuronal lineage and developmental stage. In mammals, Mn brain concentrations are increased 3 fold before toxic responses occur (Erikson et al., 2007; Molina et al., 2011) and normal brain function occurs at levels corresponding to ~20 to ~50 μM Mn, neurotoxic responses begin to occur at concentrations of ~60 to ~150μM Mn (Bowman and Aschner, 2014). Our study captures some of these ranges of sub-threshold and threshold cytotoxic levels, but since even the most sensitive LC50 value is above 500μM Mn, this suggests that Mn cytotoxicity (cell death) is not a driving factor at threshold level in vivo Mn neurotoxicity. This is consistent with minimal cytotoxicity observed in humans exposed to Mn. The goal of this study was to assess levels of Mn exposure associated with cytotoxicity to enable future studies in human neuronal models at toxicologically relevant levels with an understanding of the degree of cell death expected. However, cytotoxicity relates to relative amount of Mn taken up by cells, thus a change in cytotoxicity is likely related to a change in total Mn accumulation.

In addition, we have discovered that the HD genotype previously linked to resistance to Mn cytotoxicity, can also be associated with increased sensitivity to Mn cytotoxicity or have minimal impact depending on the specific neuronal lineage. Thus, consistent with the selectivity of the human Mn status phenotype in HD patients and model systems, cellular phenotype and state can influence not only how cells handle Mn under neurotoxic conditions but how genetic modifiers modify Mn transport and homeostatic processes. In conclusion, our findings may provide insight into therapeutic strategies for diseases in which Mn has been shown to play a role such as HD, especially through specific lineage-targeted interventions.

Funding

Supported by the United States National Institutes of Health (NIH) R01 ES010563 (ABB, MA), R01 ES016931 (ABB), and the VBI Scholars Program (PJ).

Declaration of Competing Interest

The authors declare no competing interests.

Acknowledgements

The authors thank Dr. Vivian Gama for her careful review and insightful comments for this article. We would also like to thank Dr. Anna Pfalzer, Dr. Bingying Han, Miles Bryan, Kyle Horning, Rachana Nitin, and Jordyn Wilcox for technical expertise and for thoughtful assistance with experimental design and interpretation.

Appendix A. Supplementary data

Supplementary material related to this article can be found, in the online version, at doi:https://doi.org/10.1016/j.neuro.2019.09.007.

References

Butterworth, J., 1986. Changes in nine enzyme markers for neurons, glia, and endothelial cells in agonal state and Huntington's disease caudate nucleus. J. Neurochem. 47, 583–587.
Erikson, K.M., Aschner, M., 2003. Manganese neurotoxicity and glutamate-GABA interaction. Neurochem. Int. 43, 475–480.
Bowman, A.B., Kwakye, G.F., Hernández, E., Aschner, M., 2011. Role of manganese in neurodegenerative diseases. J. Trace Elem. Med. Biol. 25, 191–203. https://doi.org/10.1016/j.jtemb.2011.08.144.
Krebs, N., et al., 2014. Assessment of trace elements in human brain using inductively coupled plasma mass spectrometry. J. Trace Elem. Med. Biol. 28, 1–7. https://doi.org/10.1016/j.jtemb.2013.09.006.
Ramos, P., et al., 2014. Anatomical region differences and age-related changes in copper, zinc, and manganese levels in the human brain. Biol. Trace Elem. Res. 161, 190–201. https://doi.org/10.1007/s12011-014-0093-6.
Prohaska, J.R., 1987. Functions of trace elements in brain metabolism. Physiol. Rev. 67, 858–901.
Aschner, M., Guilarte, T.R., Schneider, J.S., Zheng, W., 2007. Manganese: recent advances in understanding its transport and neurotoxicity. Toxicol. Appl. Pharmacol. 221, 131–147. https://doi.org/10.1016/j.taap.2007.03.001.
Pharmacol, C.-J., 1837. On the effects of black oxide of manganese when inhaled into the lungs. Br. Ann. Med. Pharmacol.
Guilarte, T.R., 2010. Manganese and Parkinson's disease: a critical review and new findings. Environ. Health Perspect. 118, 1071–1080. https://doi.org/10.1289/ehp.0901748.
Benedetto, A., Au, C., Aschner, M., 2009. Manganese-induced dopaminergic neurodegeneration: insights into mechanisms and genetics shared with Parkinson's disease. Chem. Rev. 109, 4862–4884. https://doi.org/10.1021/cr800536y.
Coetzee, D.J., et al., 2016. Measuring the impact of manganese exposure on children's neurodevelopment: advances and research gaps in biomarker-based approaches. Environ. Health 15, 91. https://doi.org/10.1186/s12940-016-0174-4.
Erikson, K.M., Shihabi, Z.K., Aschner, J.L., Aschner, M., 2002. Manganese accumulates in iron-deficient rat brain regions in a heterogeneous fashion and is associated with neurochemical alterations. Biol. Trace Elem. Res. 87, 143–156. https://doi.org/10.1385/BTER:87:1-3:143.
O'Neal, S.L., Zheng, W., 2015. Manganese toxicity upon overexposure: a decade in review. Curr. Environ. Health Rep. 2, 315–328. https://doi.org/10.1007/s40572-015-0056-x.
Shan, Z., et al., 2016. U-shaped association between plasma manganese levels and type 2 diabetes. Environ. Health Perspect. 124, 1876–1881. https://doi.org/10.1289/EHP176.
Pfalzer, A.C., Bowman, A.B., 2017. Relationships between essential manganese biology and manganese toxicity in neurological disease. Curr. Environ. Health Rep. 4, 223–228. https://doi.org/10.1007/s40572-017-0136-1.
Ericson, J.E., et al., 2007. Prenatal manganese levels linked to childhood behavioral disinhibition. Neurotoxicol. Teratol. 29, 181–187. https://doi.org/10.1016/j.ntt.2006.09.020.
Lucchini, R.G., et al., 2012. Tremor, olfactory and motor changes in Italian adolescents exposed to historical ferro-manganese emission. Neurotoxicology 33, 687–696. https://doi.org/10.1016/j.neuro.2012.01.005.
Ode, A., et al., 2015. Manganese and selenium concentrations in umbilical cord serum and attention deficit hyperactivity disorder in childhood. Environ. Res. 137, 373–381. https://doi.org/10.1016/j.envres.2015.01.001.
Dorman, D.C., et al., 2000. Neurotoxicity of manganese chloride in neonatal and adult CD rats following subchronic (21-day) high-dose oral exposure. J. Appl. Toxicol. 20, 179–187.
Fechter, L.D., 1999. Distribution of manganese in development. Neurotoxicology 20, 197–201.
Eriksson, H., Gillberg, P.G., Aquilonius, S.M., Hedstrom, K.G., Heilbronn, E., 1992. Receptor alterations in manganese intoxicated monkeys. Arch. Toxicol. 66, 359–364.
Normandin, L., Hazell, A.S., 2002. Manganese neurotoxicity: an update of pathophysiologic mechanisms. Metab. Brain Dis. 17, 375–387.
Guilarte, T.R., et al., 2006. Nigrostriatal dopamine system dysfunction and subtle motor deficits in manganese-exposed non-human primates. Exp. Neurol. 202, 381–390. https://doi.org/10.1016/j.expneurol.2006.06.015.
Trumbo, P., Yates, A.A., Schlicker, S., Poos, M., 2001. Dietary reference intakes: vitamin A, vitamin K, arsenic, boron, chromium, copper, iodine, iron, manganese, molybdenum, nickel, silicon, vanadium, and zinc. J. Am. Diet. Assoc. 101, 294–301. https://doi.org/10.1016/S0002-8223(01)00078-5.
Bichell, T.J., et al., 2017. Reduced bioavailable manganese causes striatal urea cycle pathology in Huntington's disease mouse model. Biochim. Biophys. Acta. https://doi.org/10.1016/j.bbadis.2017.02.013.
Cordova, F.M., et al., 2013. Manganese-exposed developing rats display motor deficits and striatal oxidative stress that are reversed by Trolox. Arch. Toxicol. 87, 1231–1244. https://doi.org/10.1007/s00204-013-1017-5.
Fu, H., Chen, W., Yu, H., Wei, Z., Yu, X., 2016. The effects of preweaning manganese exposure on spatial learning ability and p-CaMKIIα level in the hippocampus. Neurotoxicology 52, 98–103. https://doi.org/10.1016/j.neuro.2015.11.013.
Su, C., et al., 2016. Chronic exposure to manganese sulfate leads to adverse dose-dependent effects on the neurobehavioral ability of rats. Environ. Toxicol. 31, 1571–1579. https://doi.org/10.1002/tox.22161.
Wexler, N.S., 2004. Venezuelan kindreds reveal that genetic and environmental factors modulate Huntington's disease age of onset. Proc. Natl. Acad. Sci. U. S. A. 101, 3498–3503.

Correia, K., et al., 2015. The genetic modifiers of motor OnsetAge (GeM MOA) website: genome-wide association analysis for genetic modifiers of huntington's disease. J. Huntingtons Dis. 4, 279–284. https://doi.org/10.3233/JHD-150169.
Friedman, J.H., Trieschmann, M.E., Myers, R.H., Fernandez, H.H., 2005. Monozygotic twins discordant for Huntington disease after 7 years. Arch. Neurol. 62, 995.
Horning, K.J., Caito, S.W., Tipps, K.G., 2015. Manganese is essential for neuronal health. Annu. Rev. Nutr. https://doi.org/10.1146/annurev-nutr-071714-034419.
Tidball, A.M., et al., 2015. A novel manganese-dependent ATM-p53 signaling pathway is selectively impaired in patient-based neuroprogenitor and murine striatal models of Huntington's disease. Hum. Mol. Genet. 24, 1929–1944. https://doi.org/10.1093/hmg/ddu609.
Tidball, A.M., et al., 2016. Genomic instability associated with p53 knockdown in the generation of Huntington's disease human induced pluripotent stem cells. PLoS One 11, e0150372. https://doi.org/10.1371/journal.pone.0150372.
Chambers, S.M., et al., 2009. Highly efficient neural conversion of human ES and iPS cells by dual inhibition of SMAD signaling. Nat. Biotechnol. 27, 275–280.
Neely, M.D., et al., 2012. DMH1, a highly selective small molecule BMP inhibitor promotes neurogenesis of hiPSCs: comparison of PAX6 and Sox1 expression during neural induction. ACS Chem. Neurosci. 3, 482–491.
Di Pardo, A., et al., 2017. Defective Sphingosine-1-phosphate metabolism is a druggable target in Huntington's disease. Sci. Rep.-U.k. 7, 5280. https://doi.org/10.1038/s41598-017-05709-y.
Shi, Y., Kirwan, P., Livesey, F.J., 2012. Directed differentiation of human pluripotent stem cells to cerebral cortex neurons and neural networks. Nat. Protoc. 7, 1836–1846. https://doi.org/10.1038/nprot.2012.116.
Brown, J.A., et al., 2016. Metabolic consequences of inflammatory disruption of the blood-brain barrier in an organ-on-chip model of the human neurovascular unit. J. Neuroinflamm. 13, 306. https://doi.org/10.1186/s12974-016-0760-y.
Bryan, M.R., et al., 2017. Phosphatidylinositol 3 kinase (PI3K) modulates manganese homeostasis and manganese-induced cell signaling in a murine striatal cell line. Neurotoxicology. https://doi.org/10.1016/j.neuro.2017.07.026.
Kriks, S., et al., 2011. Dopamine neurons derived from human ES cells efficiently engraft in animal models of Parkinson's disease. Nature 480, 547–551. https://doi.org/10.1038/nature10648.
Neely, M.D., Davison, C.A., Aschner, M., Bowman, A.B., 2017. From the cover: manganese and rotenone-induced oxidative stress signatures differ in iPSC-Derived human dopamine neurons. Toxicol. Sci. 159, 366–379. https://doi.org/10.1093/toxsci/kfx145.
Kumar, K.K., et al., 2014. Cellular manganese content is developmentally regulated in human dopaminergic neurons. Sci. Rep. 4, 6801. https://doi.org/10.1038/srep06801.
Kwakye, G.F., Li, D., Kabobel, O.A., Bowman, A.B., 2011a. Cellular fura-2 manganese extraction assay (CFMEA). Curr. Protoc. Toxicol. 12 (18), 11–12.
Kwakye, G.F., Li, D., Bowman, A.B., 2011b. Novel high-throughput assay to assess cellular manganese levels in a striatal cell line model of Huntington's disease confirms a deficit in manganese accumulation. Neurotoxicology 32, 630–639.
Joshi, P., Neely, M.D., Bowman, A.B., 2018. In: Rasmussen, Theodore P. (Ed.), Stem Cells in Birth Defects Research and Developmental Toxicology. John Wiley & Sons, Inc. Ch. Chapter 7, 159-171.
Williams, B.B., et al., 2010a. Disease-toxicant screen reveals a neuroprotective interaction between Huntington's disease and manganese exposure. J. Neurochem. 112, 227–237. https://doi.org/10.1111/j.1471-4159.2009.06445.x.
Williams, B.B., et al., 2010b. Altered manganese homeostasis and manganese toxicity in a Huntington's disease striatal cell model are not explained by defects in the iron transport system. Toxicol. Sci. 117, 169–179. https://doi.org/10.1093/toxsci/kfq174.
Guilarte, T.R., Gonzales, K.K., 2015. Manganese-induced parkinsonism is not idiopathic parkinson's disease: environmental and genetic evidence. Toxicol. Sci. 146, 204–212. https://doi.org/10.1093/toxsci/kfv099.
Kwakye, G.F., Paoliello, M.M., Mukhopadhyay, S., Bowman, A.B., Aschner, M., 2015. Manganese-induced Parkinsonism and Parkinson's disease: shared and distinguishable features. Int. J. Environ. Res. Public Health 12, 7519–7540. https://doi.org/10.3390/ijerph120707519.
Erikson, K.M., Dorman, D.C., Lash, L.H., Aschner, M., 2007. Manganese inhalation by rhesus monkeys is associated with brain regional changes in biomarkers of neurotoxicity. Toxicol. Sci. 97, 459–466. https://doi.org/10.1093/toxsci/kfm044.
Molina, R.M., et al., 2011. Ingestion of Mn and Pb by rats during and after pregnancy alters iron metabolism and behavior in offspring. Neurotoxicology 32, 413–422. https://doi.org/10.1016/j.neuro.2011.03.010.
Bowman, A.B., Aschner, M., 2014. Considerations on manganese (Mn) treatments for in vitro studies. Neurotoxicology 41, 141–142. https://doi.org/10.1016/j.neuro.2014.01.010.